CHALMERS
UNIVERSITY OF TECHNOLOGY

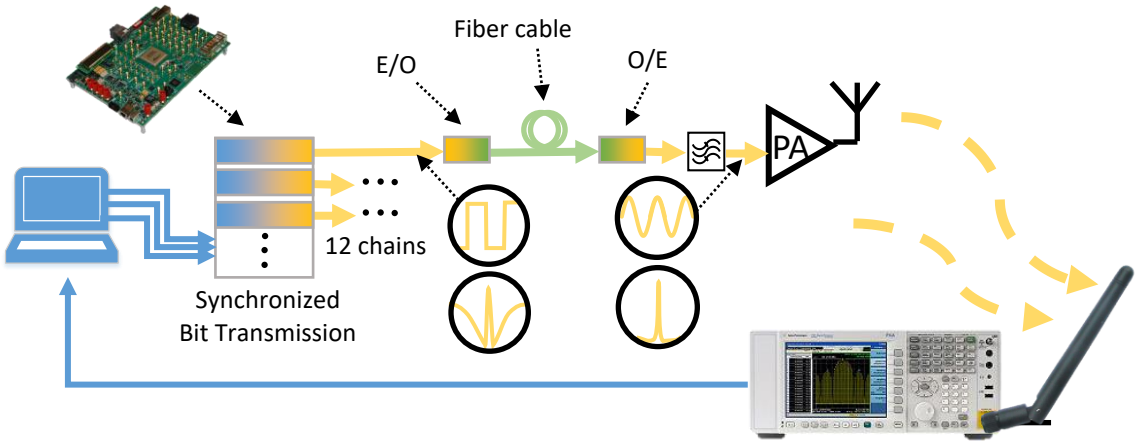

Implementing Distributed MIMO

With Sigma-Delta-over-Fiber

Master's thesis in Communication Engineering

Martin Dahlgren

Department of Electrical Engineering

CHALMERS UNIVERSITY OF TECHNOLOGY

Gothenburg, Sweden 2018

Implementing Distributed MIMO

With Sigma-Delta-over-Fiber

Martin Dahlgren

Implementing Distributed MIMO
With Sigma-Delta-over-Fiber
Martin Dahlgren

Department of Electrical Engineering
Chalmers University of Technology
SE-412 96 Göteborg
Sweden

In collaboration with:
Department Microtechnology and Nanoscience,
Chalmers University of Technology
&
Ericsson Research

ABSTRACT

MIMO systems have revolutionized wireless communication the last decade, pushing the limits of achievable data rates in an increasingly crowded spectrum. Traditionally, MIMO antennas are located within a few wavelengths distance from each other. In such setups high spatial correlation in both small-scale and shadow fading limits the achievable capacity.

However, in this thesis a Distributed MIMO testbed is designed and implemented, where 12 transmit antennas are spread out over the cell area. Theoretically predicted improvements of such an antenna set-up in terms of increased coverage is experimentally verified in an indoor environment for a single receiver.

To enable the increased separation between the transmit antennas, Sigma-Delta-over-Fiber (SDoF) is used for the antenna fronthaul, supporting distances of hundreds of meters between the remote antennas. This enables phase-coherent transmission from spatially distributed antennas. By using SDoF all local oscillators as well as the computational complexity is moved from the remote-radio heads to a central unit. To the author's knowledge this is the first implementation of D-MIMO using Sigma-Delta-over-Fiber.

ACKNOWLEDGEMENTS

I had the great fortune to work with some very talented people through this thesis, without them I could not have done this work.

I want to thank Ibrahim Can Sezgin for a lot of time spent supervising and helping me with all parts of the thesis, especially regarding hardware design and assembly of which I knew very little at the project start. I also want to thank Christian Fager and Thomas Eriksson from Chalmers as well as Christina Larsson and Mikael Coldrey from Ericsson Research for their interest and vital insights throughout the project.

Lastly I want thank Alexander Grahn for helping me with measurements and giving support and motivation during the entire thesis work.

TABLE OF CONTENTS

1 INTRODUCTION

The use of wireless data continues to increase each year and customers keep expecting better coverage and higher throughput. To support this development and meet customer demands wireless technology companies are always researching new ways to increase network capacity while lowering costs.

In this thesis two new interesting technologies are explored which might be used in future communication systems. Distributed MIMO has been researched for many years but has yet been hard to implement in a commercial system. This is due to problems of achieving phase coherent transmission from separated transmitters. Another new technology is Sigma-Delta-over-Fiber which is used to transmit analog radio signals through digital fiber links with low delays. This technology could create the possibility to meet the requirements needed for implementing Distributed MIMO for low costs.

In this thesis a testbed was implemented demonstrating this concept in an indoor environment. This introduction chapter presents the thesis aim as well as an overview of some of the system components used.

1.1 DISTRIBUTED MIMO

The current development of wireless communication has been towards adding more antennas collaborating for better performance in terms of higher total throughput and power efficiency. This technology with many transmit antennas as well as receiver antennas is called Multiple Input – Multiple Output (MIMO). By various signal processing means at either receiver or transmitter the spectral efficiency can be increased in the system.

MIMO systems generally have all base station antennas co-located for example in an antenna array with short distance in between compared to the wavelength. The nearness of the base station antennas creates two problems. One is high correlation in path loss and shadow fading to the base station antennas as seen from a mobile device. That means if a mobile device experiences a wireless channel with high attenuation from one of the base station antennas there is a high probability of experiencing high attenuation to also the other base station antennas.

The other issue is the small scale fading diversity which sets limits on the number of simultaneous spatial streams possible. If the channels to all receiving antennas are too similar it is not possible to separate different streams, and reach high MIMO gains, even when the channels conditions to each antenna are good when considered independently [1]. This can also be explained as having a low rank of the channel matrix.

These properties of the system will likely be more favorable if the transmit antennas are spatially distributed and not mounted on the same antenna array. This would increase performance in terms of both spectral efficiency and outage probability [2, 3]. The idea is illustrated in Figure 1-1; the base station antennas are separated into what will here be called Remote-Radio Heads (RRH). The separation could be between a few meters to multiple kilometers. These RRHs work synchronized as a single, but distributed, base station enabling joint transmission to the receivers.

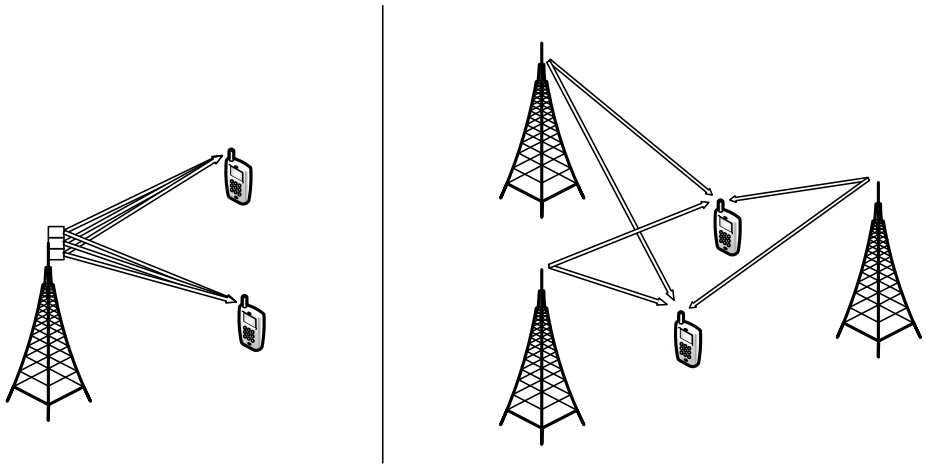

Figure 1-1: Illustration of the difference between co-located and D-MIMO, both employing 3x2 MIMO.

This set up with spatially distributed antennas is called *Distributed MIMO* (D-MIMO), *Cooperative MIMO*, *Network MIMO* etc. The name *cell-free MIMO* is sometimes used, implying an access network topology without traditional cell boundaries.

The problem with having the MIMO antennas separate are that the tight constraints on carrier phase synchronization and signal quality which are needed for coherent transmission are hard to reach. It is possible to have multi-antenna systems without phase coherent transmission, however the possible gains of such systems are lower [4].

To achieve coherent transmission there are multiple previously suggested methods, however these leads to increased system complexity. Most methods involve keeping the Local Oscillators used for carrier waves synthesis synchronized between the RRHs. A proposed solution to make the RRH simple - removing the need for separate D/A converters, digital hardware and local oscillators there - is to transmit the waveform already modulated at carrier frequency through a wired backhaul. This moves complex signal processing from the RRHs to a centralized unit [5].

1.1.1 Previous Work

There are already demonstrated implementations of D-MIMO, e.g. Artemis' pCell™ which creates a virtual mobile cell to each connected user and supports established protocols such as LTE and 802.11. They claim a 35x increase in spectral efficiency already for unmodified LTE devices compared to traditional base stations. [6]. There are also similar demonstrations, for example by Ericsson [7].

In the testbed presented in [8], multiple secondary access points have individual local oscillators but the phase drifts of these are tracked by following a calibration signal transmitted from a master access point. In [9] the access point phase offsets are additionally tracked from uplink transmissions.

Also radio over fiber systems have previously been used to implement distributed MIMO testbeds however using analog techniques instead of sigma-delta based. For example [3] did channel measurements using a fiber based system, however no joint transmission was done in that implementation. Capacity was only analytically determined from estimated channels.

1.2 Sigma-Delta over Fiber

There are various solutions for transferring the signal that is to be transmitted at a RRH from a central processing unit. We consider an alternative where it is done through an optical wired backhaul.

A lot of research has been done in analog radio over fiber where an optical signal is modulated by the RF signal; it could be at baseband, RF frequency or an intermediate frequency (IF). Doing so has a number of problems in terms of power loss, nonlinearities and intermodulation distortion (IMD). [5]

A way to mitigate this is to digitally transmit the RF signal samples to the RRH over fiber (Digital Radio over Fiber, D-RoF), and have a D/A-converter at the RRH reconstructing the RF signal. This option still requires one to employ digital hardware at each radio head, and for phase coherent transmission the oscillators has to be synchronized.

A third solution, which is investigated in this project, is to transmit Sigma-Delta modulated RF-signals over fiber from the base station central unit to the antenna heads (Sigma Delta over Fiber, SDoF). The key to this technology is the Sigma-Delta modulator which takes an already upconverted waveform and transforms it to one that is more suitable to be transmitted on a fiber cable. The signal is transferred on a fiber cable and recovered using only a band pass filter around carrier frequency. More background on the Sigma-Delta converter is in section 1.5

SDoF works over long distances and removes the need for separate frequency converters and D/A converters at each RRH. It is also more resilient to the issues with traditional analog radio over fiber in terms of IMD and limited dynamic range since the constraints on linearity are reduced [5]. Thus for implementing a downlink only a single clock source is required at the transmit side.

The MC2 department at Chalmers University of Technology is researching this method calling it *all-digital radio-over-fiber*. This is done with a commercially available FPGA platform, ideal for easily deployed D-MIMO systems with a large number of Remote-Radio Heads.

1.3 Thesis Aim and Contribution

The aim of the thesis was to implement a distributed MIMO link using Sigma Delta over Fiber to transmit signal from the central processing unit to Remote-Radio Heads. The system used 12 transmit antennas. After development of the system performance tests were done in terms of quality and power of received signal. Comparisons are also made between co-located MIMO and distributed MIMO setups.

The implementation uses the *all-digital radio-over-fiber* solution at Chalmers. Some system components were not available at the project start: These include antennas, amplifier PCBs, amplifier power sources and communication signal processing software. Such components were developed, manufactured and/or chosen as necessary.

To the author's knowledge there has been no previous implementations of distributed MIMO using Sigma-Delta over Fiber.

1.4 Scope

Focus was on system design rather than of details of Sigma-Delta modulation or on any other individual system component. Also there was no goal that the demonstration system would be useful as a functioning communication system, there e.g. might be considerable delay between channel state estimation and transmission during which it is required that the channel remains static. Influence of fading in a distributed antenna setup was therefore not investigated. The system is rather a proof of concept.

The communication link only has a downlink. Therefore exploiting reciprocity during Time Division Duplexing (TDD) for Channel State Information (CSI) estimation is not possible and the channel can only be estimated from downlink transmissions. There is instead an assumption of a perfect separate feedback channel, enabling channel estimation from the receiver to be used for precoding in the transmitter. In practice both the transmitter and receiver hardware were connected to the same computer.

1.5 Sigma Delta Modulation

This section presents a review of Sigma Delta modulation. A more thorough and mathematically rigorous description can be found in for example [10]. The Sigma Delta modulator was developed in the 1960s and was originally developed to create high resolution A/D converters from low resolution but high sample rate A/D converters. There are different names for it: Sigma-Delta (ΣΔ), Delta-Sigma (ΔΣ) or more generally noise-shaping modulators.

The function can also be the opposite – to create a high resolution analog signal from a low resolution D/A converter. This is what will be done in this project. We will digitally modulate a low bandwidth signal with a sigma delta converter to create a binary signal. This binary sequence will be transferred over some distance and the original signal is recovered using only a filter.

To create some intuition to how it works consider a signal containing only low frequencies compared to the sample rate. This case is shown in Figure 1-2 where a low frequency signal is Sigma-Delta modulated to a binary signal. By only applying a low pass filter the original signal is recovered. Here it is clear to see that the relative count of high to low bits determines the signal value. One way of viewing ΣΔ is that it realizes *noise-shaping*, meaning that the quantization noise of a low resolution quantizer is pushed away from the frequencies of interest.

The signal quality seems low in the figure, but that relates to the low OSR (oversampling ratio) of 16 used for the illustration. OSR is sampling rate compared to the signal bandwidth, or for a low pass ΣΔ the sampling rate to maximum signal frequency. The maximum achievable SQNR (Signal-to-quantization-noise ratio) for binary ΣΔ scales exponentially with OSR [10]. This illustration was for low pass Sigma-Delta however in the project band pass Sigma-Delta, where the band of interest is at a higher frequency, was used. The principle is similar, in that the quantization noise is pushed outside the band of interest and again the signal can be recovered using a band pass filter. However it is not as easy to illustrate band pass ΣΔ in time domain. Band pass ΣΔ is illustrated in frequency domain in Figure 1-3, here the oversampling ratio is 1000. The decoded symbol NMSE is -59 dB as defined in section 1.6.

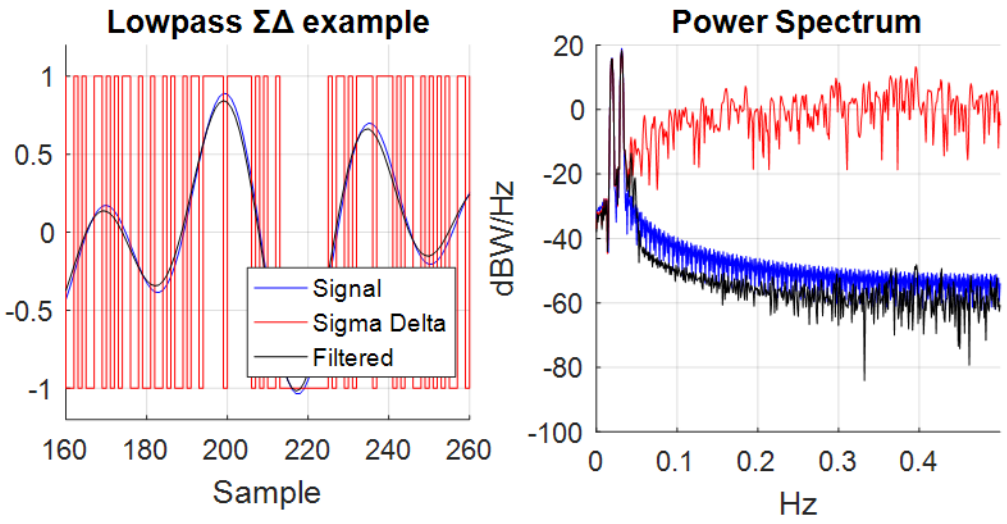

Figure 1-2: Example of bi-level low pass Sigma-Delta modulation. The ΣΔ signal as well as original and filter recovered signal is shown in time domain (left) and frequency domain (right). The signal includes two sinusoids, at 6.3% respective 4% of the Nyquist frequency. This gives an oversampling ratio of 16.

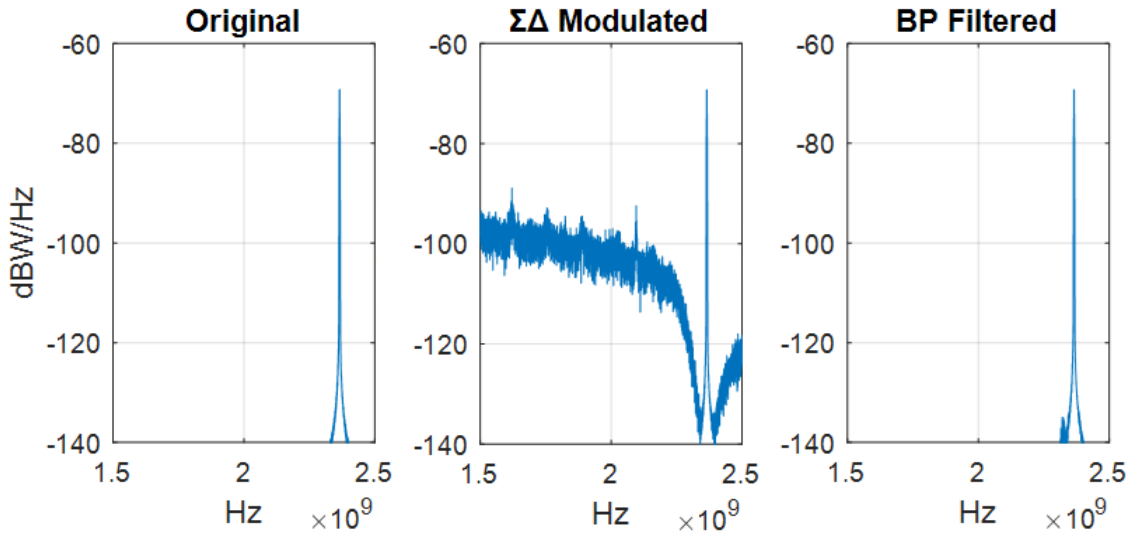

Figure 1-3: Spectrum of a QAM modulated signal at 2.365 GHz at left. Middle figure is Sigma-Delta modulated signal and right is recovered signal after band pass filter (order 400 FIR). Signal bandwidth of 5 MHz and sample rate 5 GHz is giving an oversampling ratio of 1000.

1.6 NMSE (Normalized Mean Square Error)

There are different metrics to use for quantizing signal quality. The one which will be used in this thesis is the Normalized Mean Squared Error (NMSE); where low NMSE indicates a good signal quality. This metric shows how similar two signals are by comparing the power of the difference between the signals to the reference signal power. It can be used both for waveforms and constellation points, however it does not take time shift between signals into account so for two signals which are identical but time-shifted the NMSE might be high.

The definition of NMSE that is used in thesis is as follows where x is a reference signal to which one compares y:

$$\text{NMSE} = 10 \cdot \log_{10}\left(\frac{\|x-y\|_2^2}{\|x\|_2^2}\right)[\text{dB}] \quad (1)$$

where $\|\cdot\|_2$ is the Euclidean norm.

NMSE can be useful in a communication system if y is a received signal when x was transmitted. The difference between x and y could e.g. be noise in the receiver or non-idealities in any part of the signal chain as well as interference signals received.

For getting a notion of NMSE values consider a communication system where the difference between and received signal is white Gaussian noise within the signal bandwidth. In this case an NMSE of -15 dB will be enough to transmit a 16-QAM signal with less than 0.1 % bit errors. Already with an NMSE of 0 dB, i.e. the same amount of noise power as signal power, a binary signal can be transmitted with a bit error probability below 10 %. In general when experiencing lower NMSE more data can be transmitted per second given a requirement on bit error integrity. [11]

2 HARDWARE IMPLEMENTATION

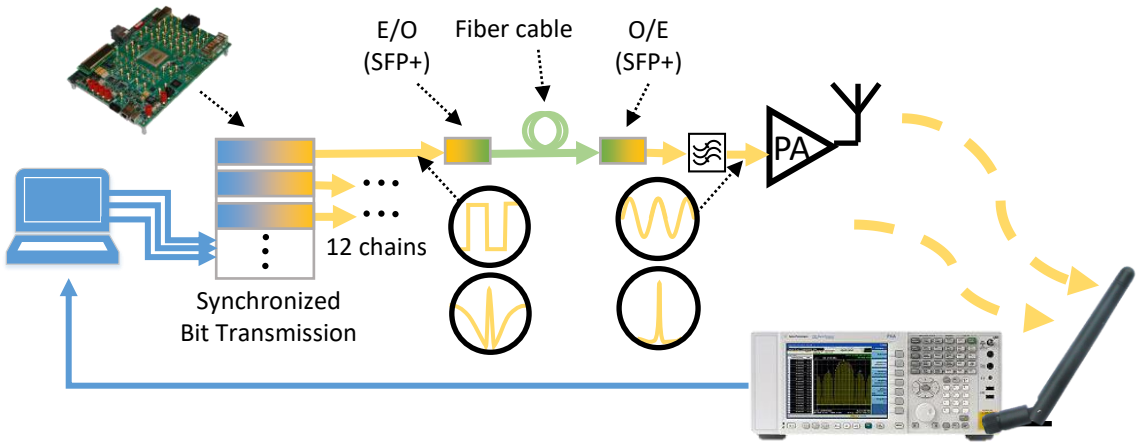

Figure 2-1: Signal Path overview. A signal is digitally generated and transmitted as a binary Sigma-Delta modulated signal. It is recovered at the BP filter, transmitted over air and received using a spectrum analyzer in IQ-mode. E/O and O/E refers to electrical to optical respectively optical to electrical converters.

To enable the tests both hardware and software parts had to be developed. This chapter will focus on the system architecture and the hardware implementation. Details of the software implementation as well as used algorithms will be focused on in Chapter 3 but there is a lot of overlap between the parts. Therefore, the chapter will start with a System Overview.

The idea is to realize D-MIMO with Sigma Delta over Fiber. The test system overview is showed in Figure 2-1. 12 signal paths are provided to 12 spatially distributed antennas. Note the lack of analog mixers at the Remote-Radio Head side.

A PC performs all signal processing: generating pilot as well as data sequences and decoding received IQ waveforms from the spectrum analyzer. The transmitted signals are Sigma-Delta encoded to bit patterns and transmitted synchronized from a bit transmitter.

There are 12 synchronized out ports from the bit transmitted. Each signal is passed through an Electrical/Optical converter (SFP+) and a fiber cable. In this set up 30 meters long fiber cables were used, however longer cables of up to a few hundred meters are supported. The optical signal is converted back to an electrical signal in another SFP+. The signal is here still bi-level and ideally should be unaffected by the optical components. By a very narrowband band pass filter around center frequency the intended waveform is recovered and then amplified using a power amplifier.

12 synchronized radio signals are then transmitted to the receiver by patch antennas. The receiver in this case is an Agilent® PXA Signal Analyzer which is feeding IQ data back to the computer doing all processing. The carrier frequency is at all tests 2.365 GHz, because filters and radio license were acquired for only that radio band.

Both position of the 12 transmit antennas as well as the receiver can be changed. In this way channel characteristics in terms of attenuation and relative phase during different setups and positions can be measured.

2.1 BIT TRANSMITTER

The bit pattern generator used is an Altera® Stratix® V GT Transceiver Signal Integrity Development Kit. This is running a custom firmware and is equipped with a custom[1] expansion board giving a total capacity of 12 synchronized binary outputs.

Each output is interfaced with differential SMA connectors. In the used configuration the bitrate is 5 Gigabits per second. These bits are continuously read from an inbuilt memory with 12 banks – one for each

output. The transmitted bit sequence is looped infinitely if no new data is uploaded. This uploading is done through a USB interface and a MATLAB function has been written to do the uploading.

In current configuration the memory banks are 240,000 bits long, 5Gbit/s transmission gives that each output loops an up to 48μs long signal. Uploading of new data to transmit takes approximately 14 seconds. To ensure a stable bitrate there is an external reference clock signal provided from a signal generator.

When transmitting a Sigma-Delta modulated QAM signal a symbol level NMSE of -28 dB was acquired. Applying the Shannon-Hartley theorem [11] the theoretical maximum capacity is about 9.3 [bits/s/Hz] given this NMSE. Reasons for signal degradation compared to simulated Sigma Delta could be phase noise from that the bitrate is not perfectly constant. Also, the output cannot be exactly bi-level since the bandwidth is limited in a physical system, therefore nonlinearities in the optical equipment can distort the signal. The frequency error in was in measurements approximated to 100 Hz using the method described in section 3.1.2.

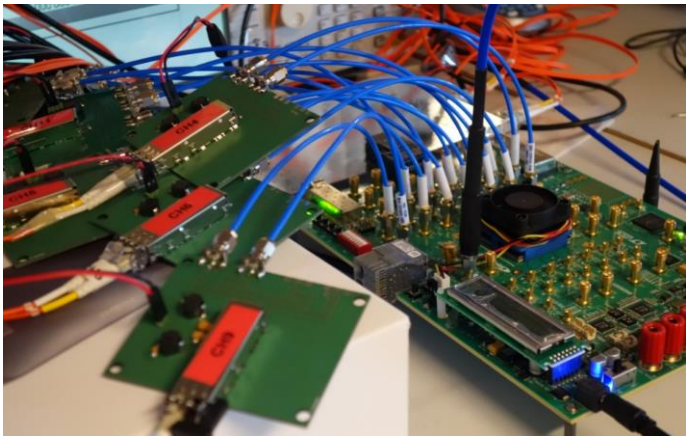

Figure 2-2: Bit transmitter in background with Electrical/Optical converters in foreground. Orange cable is the fiber cable towards the remote-radio heads. From this board phase coherent bi-level signals are transmitted.

2.2 FIBER OPTICS

The system components that enables distributed MIMO in terms of the long distance between transmitters is the fiber-optical link. The reason for Sigma Delta modulation was only to create a signal that is easy to transmit over a fiber cable, with nonlinear behavior.

Each output from the bit transmitter is connected through an electrical to optical converter to an OM4 fiber cable of length 30 meters and connected back to an optical to electrical converter at the RRH. For E/O and O/E conversion commercially available SFP+ (Enhanced Small Form-factor Pluggable) optical transceivers are used. These contains VCSELs (Vertical-Cavity Surface-Emitting Lasers) and photo-diodes.

The SFP+ boards support an up to 10 Gbit/s data rate. Each requires a 3.3 Volt power source and at the central processing side this is provided by a conventional lab power supply however at the RRH this is provided my more portable small form batteries, more about this in section 2.3.4. The SFP + boards are mounted on custom PCBs[1].

At a test of transmitting a communication signal through the bit transmitter and the entire electrical-optical-electrical signal path an NMSE of -28 dB was measured. Comparing to the signal quality at the bit transmitter output this means the fiber optics does not add any significant signal degradation.

The power of the signal at the SFP+ output, measured only at the interesting band around carrier frequency, i.e. not including the quantization noise, was determined to be -8.5 dBm.

[1] Designed by Ibrahim Can Sezgin.

2.3 RF Front Ends and Antennas

What is meant with RF Front Ends here are the analog filter as well as amplifiers at the Remote-Radio Heads. The analog band pass filter is needed to remove the quantization noise and recover intended radio signal (consider the quantization noise in Figure 1-3). As mentioned the bi-level signal contains the original signal already upconverted to carrier frequency, so no analog mixer is required at the RRH.

This hardware development consisted of choosing components, designing and assembling PCBs as well as ensuring correct functionality. It was done in a two phase process. At first stage a small number of PCBs containing amplifiers as well as PCBs housing filters were manufactured so that performance of the individual components could be tested individually. When that was shown to work 12 new PCB designs were manufactured containing both filter and amplifier on a single PCB. This reduced losses in connectors and enabled easier handling. The final PCB layouts are shown in Figure 2-3.

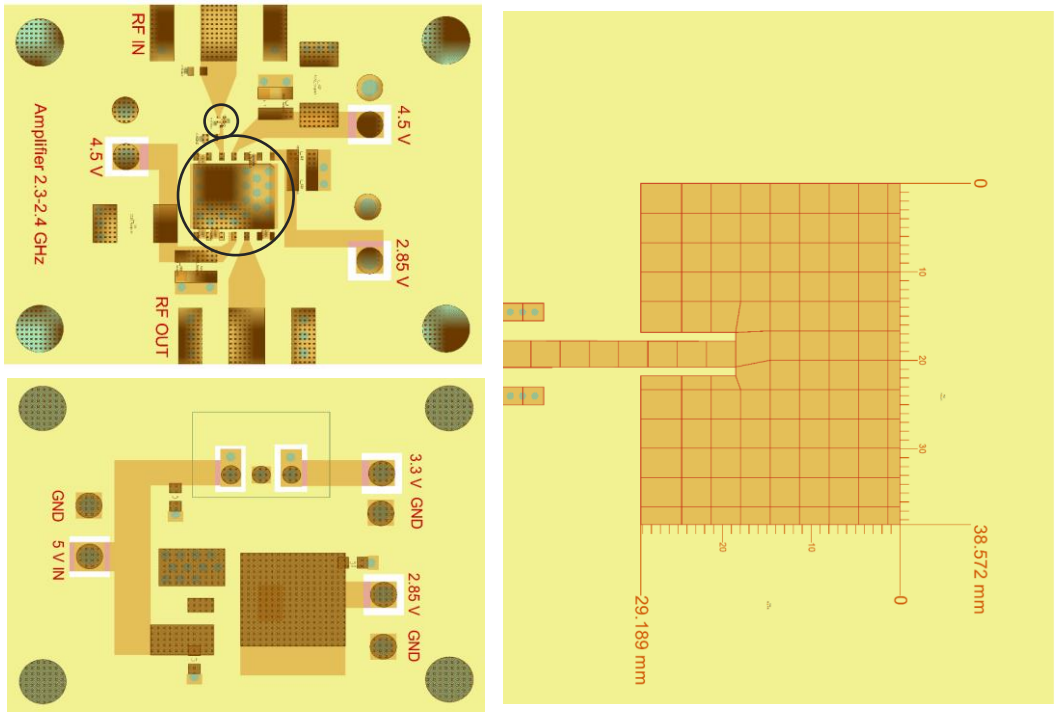

Figure 2-3: The final edition of the three designed PCB layouts. Top-left is amplifier and filter PCB. Bottom-left is voltage regulation board. To the right is the patch antenna. The small and large circle on the amplifier PCB layout marks the placement of the band pass filter respectively the amplifier.

2.3.1 Filter

The bandpass filter used is the commercial filter Qorvo® 885075. It is a bulk-acoustic-wave (BAW) filter and was chosen for having a very narrow passband. It has less than 2 dB loss in the 2.3 - 2.4 GHz passband and at least 20 dB rejection in the stop band (10 - 2170 and 2427 - 7200 MHz).

It is sold as a SMD (Surface Mount Device) component and requires mounting on a PCB. Likely it is intended to be used in mobile devices since it has a small form factor of 1.1x0.9x0.5 mm with 5 underneath connectors. The data sheet recommended inductors of 3.4 nH on RF input and output which were added.

2.3.2 Amplifier

To be able to have a separation of transmit antennas such that D-MIMO can be useful a high output power was needed from each antenna.

Table 1: Link Budget Parameters

Receiver Noise Figure	5 dB
Ambient temperature	290 K
Signal Bandwidth	10 MHz
Signal carrier frequency	2.365 GHz
Required SNR	20 dB
Distance	40 meters
Antenna gains (Tx and Rx)	0 dB
Margin	30 dB

The parameters of Table 1 were used for a link budget calculation, these parameters were chosen just to get a sense of needed amplification. For example the exact antenna gains are not known. Link budget calculations were done using the free space path loss model in Appendix.

The link budget calculations showed that 23 dBm transmitted power was required. With a signal input of -8.5 dBm that results in an amplification of 31.5 dB.

The most suitable amplifier found was a 36 dB gain amplifier, a Qorvo TQP9424 being conveniently already matched to 50 Ohm input/output. Also this was available in a SMD package requiring PCB mounting. The recommended circuit from the data sheet included multiple values of capacitances from DC to ground as well as inductors from RF to ground; these were added as recommended.

The amplification in the final assembly in combination with the band pass filter was measured to be 32 dB, giving a total output power of 23.5 dBm at each transmit antenna in-port. Some spectral leakage was seen, possibly also due to noise in the amplifier power supplies.

2.3.3 Microstrip Patch Antenna

A microstrip patch antenna was designed for being used at the transmitters. A patch antennas was chosen since it can be printed on a circuit board and thus is simple to manufacture. Also they have a narrow bandwidth, which is a useful property for this application when the filter possibly wouldn't be enough to completely remove the quantization noise.

A first patch antenna was designed in ADS (Keysight® Advanced Design System) according to available formulas of patch antenna dimensions. The design flow was based on very practical slides found online [12]. More descriptions of patch antennas can be found in for example [13].

The antenna performance was also simulated using the software ADS ensuring that the matching as well as resonance frequency were correct.

After production of the first antenna batch it was noticed that the center frequency was 49 MHz too low in the manufactured antenna. Because of the low antenna bandwidth that meant that almost all signal power would be lost. Reasons for the offsets could be that values of material parameters used for simulation did not match the true values.

In simulations it was tested to see which length adjustment was needed to move the center frequency 49 MHz. This was then that was compensated for in the second batch, so that in simulations the resonance frequency seemed 49 MHz too high. However the manufactured antennas had correct center frequency of about 2.365 GHz. This can be seen from the reflection coefficient (S11) which is shown in Figure 2-4.

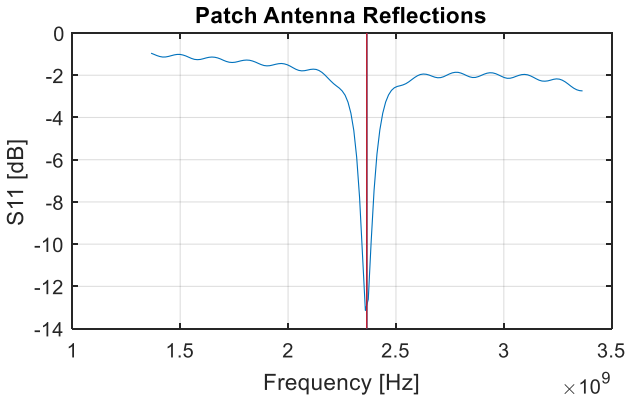

Figure 2-4: Patch antenna reflection coefficient as measured in VNA of one of the manufactured antennas in the second batch. Red line marks the center frequency of 2.365 GHz.

2.3.4 Power Source

The idea was to have the remote-radio heads be portable to enable changes of antenna placement for measurements of different scenarios.

To reach that portability each RRH had to be equipped with its own power source capable of providing power to amplifier and Electrical/Optical converters. The requirements on voltage and current were found in respective data sheet and are shown in Table 2.

Table 2: Voltage Source Requirements for each RRH

Use:	Recommended Voltage (range):	Maximum current drawn:
SFP+ E/O Converter	3.3 (3.13 – 3.46) V	160 mA
Amplifier reference voltage	2.85 (2.75 – 2.95) V	19.5 mA
Amplifier supply power	4.5 (3.6 – 5.25) V	500 mA

To provide these power a commercially available power bank was chosen. This is intended for use with for example smartphones and provides regulated 5 Volt through a USB port. The maximum current rating is 2.1 A. The energy capacity rating is 13500 mAh at 5 V. The chosen powerbank has an on/off button enabling turning off the RRH.

The amplifier supports a supply voltage of 5 Volt, so that was directly connected to the power bank. To provide the amplifier reference voltage a commercial LDO voltage regulator was used. And for the SFP+ 3.3 Volt a switching regulator was chosen.

Both these were mounted on a custom PCB together with capacitors to ground to further stabilize the voltage. The layout can be seen in Figure 2-3.

An effect was seen when the 3.3 volt regulator did not start correctly when tested with a lab power supply of 5 Volt. The voltage regulator was rated for an input power of 4.5 to 28 Volt input so 5 Volt input was at the lower input range. When the input voltage was started at a higher voltage and then lowered to 5 Volt the regulator worked at expected. Fortunately no problems were detected when used with the intended power bank. Possibly the power bank had some overshoot at start up, or there were some other lucky coincidence that made the voltage regulator work as intended with the power bank.

2.4 Final RRH Assembly

After testing the components individually the RRH were assembled into practical self-contained boxes. The only input to the box is the fiber cable, and the patch antenna sticks out on the side. There are holes for charging the power banks as well as to reach the on/off button. Figure 4-3 shows the final assembly of one of the 12 RRHs. Figure 2-5 show the 12 assembled RRHs.

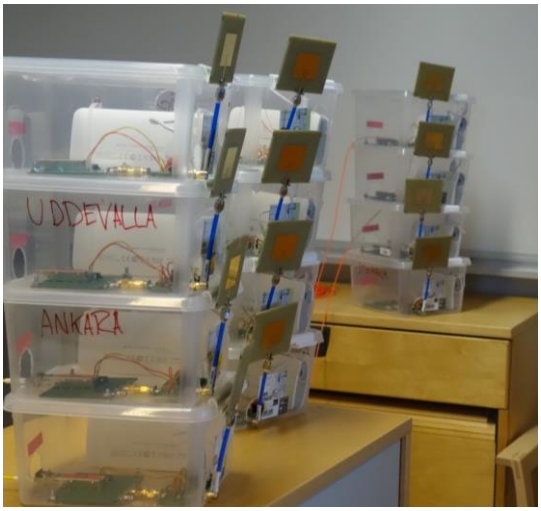

Figure 2-5: A photo of the assembled remote-radio heads. Some have been named. In this photo not all are connected by the fiber cable on the backside.

3 SIGNAL PROCESSING

To enable measurements of a communication system utilizing the Sigma-Delta over Fiber this communication system had to be implemented. To get a better understanding of and ability to fine tune parameters of the communication system it was designed from a low level in the programming language MATLAB®.

The aim of this stage of development was to design a general digital communication link transmitting symbols using Single-Carrier QAM modulation to one or more receivers. Development included corrections for radio channel non-idealities such as carrier frequency offsets and time shift.

This communication system was developed for use both with real hardware as well as in a simulated environment and made to be able to run with both. The wireless channel in this case is represented by a single MATLAB object, enabling easy adaption of the software to new uses, e.g. simulators with new channel properties, or other types of hardware.

A key point of the software development was to make it flexible to enable reuse of software parts, e.g. to have the option to adapt it to systems were the Sigma-Delta modulation is not necessary. Focus on the development was to have the system working rather than optimizing the signal processing computational time and complexity. Again the system is not designed to be used for real time processing, for a faster processing time MATLAB would not have been the ideal choice.

In this chapter a general overview of the software will be presented as well as details of interest.

3.1 SINGLE LINK

As a first step, of the communication system signal processing development, processing for a single link was implemented. This section will describe the general idea of the basic communication link implemented. The link is developed from conventionally used techniques, for more information about the basics of digital communication refer to a textbook such as [11]

In this implementation bits are transmitted over a communication link using a QAM modulated sinusoid where phase and amplitude are used to represent symbols mapping to specific bit sequences. This single link will be the building blocks of the multiantenna signal processing described in section 3.2 Multiantenna Processing.

3.1.1 Transmitter

Since the purpose of the link is to evaluate system performance bits are randomly generated. The bits are converted to complex symbol representations. These symbols are pulse shaped using a Root Raised Cosine Pulse with roll-off factor $\beta = 1$.

There were issues in the specific hardware used that appeared when transmitting with low signal power. When pulse shaping a symbol sequence the RRC puls-shaping filter delay will appear in the beginning and end of the signal. This signal part will have a low power and trigger the issues mentioned. To circumvent it some pseudorandom symbols are padded to the end and beginning of a frame so that there are no long signal segments of low average power.

The symbol rate is variable but in all tests done at 2.5 MBaud. In this case the baseband processing is done in 25 MS/s. The rate of the bit transmitter is 5 Gbit/s, therefore the baseband signal is upsampled to 5 GS/s. It is then upconverted to specified carrier frequency (at tests 2.365 GHz) using QAM.

A sinusoid is optionally added a few MHz outside the signal band to aid in frequency offset compensation (mixer LO offsets or sample rate offsets). This method of adding a sinusoid for frequency correction has the drawback compared to more complex techniques in that it will waste both power and bandwidth which could otherwise have been used for data. The advantage is simple implementation. This added sinusoid will be referred to as the frequency pilot.

After this step the data can be transmitted, either through a channel simulator or a physical channel by some hardware. At first development steps a simple channel simulator was used to debug the signal processing implementations. Then MATLAB interfaces to the bit transmitter as well as the sampling spectrum analyzer were used.

Sigma Delta Modulation

The Sigma-Delta (ΣΔ) modulation is implemented using the Delta Sigma Toolbox for MATLAB® by Richard Schreier[2]. In all tests a 2nd order band pass binary ΣΔ-modulator is used, optimized for a center frequency of 2.365GHz; but any center frequency up to the Nyquist rate is possible.

3.1.2 Receiver

At the receiver the processing is done backwards to recover the data. Receiver in this section refers to the processing of the incoming signal, either from a channel simulator or some hardware providing IQ samples. The received signal is here in baseband, with the same sample rate as was used to create the signal (25 MS/s). The first step is to roughly cut out the relevant part of the signal. Since the transmission is looped and there is a lot of margin in the receive time window it is guaranteed that the received waveform contains the transmitted signal.

CFO Compensation

There are likely frequency offsets in the communication signal chain. To recover from these a sinusoid could be included in the transmission outside the data signal band. In measurements this sinusoid was placed at 2.3695 GHz, i.e. 2 MHz outside the modulated signal bandwidth. The transmitted waveform is then

$$x_{\mathrm{T}}(n) = x_{\mathrm{data}} + \sin\left(2\pi f_{\mathrm{sine,\,Tx}} \frac{n}{f_{\mathrm{s}}}\right). \qquad (2)$$

By estimating the frequency of the sinusoid in the received waveform frequency offsets can be detected. Following is a description of the method used to estimate the sinusoid frequency of a received waveform.

[2] The Delta Sigma Toolbox is available at https://www.mathworks.com/matlabcentral/fileexchange/19-delta-sigma-toolbox

From the Fourier transform it is seen that a real time sinusoid is seen as peaks in the frequency domain at the negative and positive frequency. The received waveform is in complex baseband, here the same sinusoid is represented as a single peak.

Assuming low interference around the frequency pilot the way to estimate the frequency is to find a peak in the spectrum close to where the sinusoid should be found. The maximum was searched for in the range of ± 1 MHz around the frequency of the transmitted sinusoid. Processing is done in complex baseband since the receiver hardware already has down converted the signal.

That is if x is received signal the estimated frequency of the received frequency pilot is

$$\hat{f}_{\text{sine}} = f_{\text{carrier}} + \underset{f_{\text{sine, Tx}}-1\ [\text{MHz}] \le f \le f_{\text{sine, Tx}}+1\ [\text{MHz}]}{\text{argmax}} S_{xx}(f - f_{\text{carrier}}) \qquad (3)$$

where $f_{\text{sine, Tx}}$ is the frequency of the transmitted sinusoid, f_{carrier} the carrier frequency and $S_{xx}(f)$ the estimation of the power spectral density (PSD) in baseband.

The PSD is estimated using Welch's method with the built-in MATLAB function *pwelch(….)*. A Hamming window of the signal length is used. A parameter to the pwelch function is the frequency points of where to estimate the PSD and these were chosen linearly in the search range. It was seen that a high resolution in frequency slowed down the computation. Therefore, the frequency domain resolution was set to 0.52 kHz.

An example of the output is seen in the blue line of Figure 3-1. The low resolution makes it hard to distinguish a clear peak. Therefore, after identifying the maximum of the output, the peak was interpolated using spline interpolation with MATLAB's built in function *interp1(…)*.

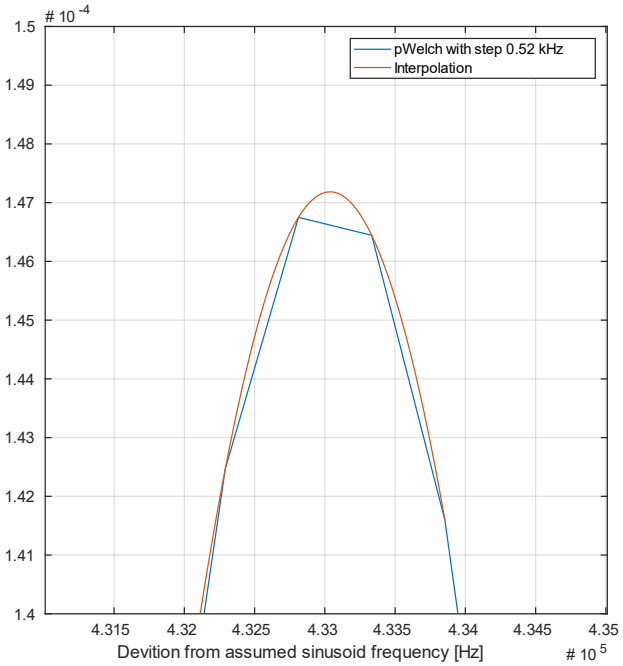

Figure 3-1: Illustration of sinusoid detection in the frequency domain. The power spectrum density of a sinusoid has a peak at the frequency of the sinusoid. To more clearly distinguish the maximum value, the curve has been interpolated.

The author does not know if the spline interpolation (as implemented in *interp1*) is an optimal choice and that it improves accuracy. However, testing indicated satisfactory results. The accuracy of this method has not been analytically determined, simulations with additive white gaussian noise showed that with SNR values of around 21 dB the CFO estimation error using this technique was consistently below 80 Hz.

Having a frequency offset in the LO of a mixer the absolute error in frequency of the pilot sinusoid would also be the offset of the carrier frequency. For example, if the frequency pilot is detected 300 kHz too high the carrier wave would also have a 300 kHz offset that needs to be corrected for.

In our system it is likely that a frequency error is instead a sample rate error. This since the data is transmitted already upconverted, so there is no LO that can have a frequency offset. There is however a clock signal to the transmitter ensuring that samples are transmitted at exactly 5 Gbit/s. A constant rate error here would also introduce a shift in the spectrum; however, that shift would not be constant over the entire spectrum. Instead the frequency error would be linearly changing over the spectrum with maximum deviation at the Nyquist rate. When the deviation of the added sinusoid is determined the shift at carrier frequency is found as

$$\Delta f_{\text{carrier}} = \left(\hat{f}_{\text{sine}} - f_{\text{sine, Tx}}\right) \cdot \frac{f_{\text{carrier}}}{f_{\text{sine, Tx}}} \tag{4}$$

This offset is then compensated for by multiplication with a complex sine of opposite frequency.

Signal Time Alignment

A simple model of the received baseband waveform is that the transmitted signal *x* has been delayed by an unknown number of samples τ, scaled by a complex scalar *h* and have added gaussian noise *N*. Then the received waveform is

$$y(n) = h \cdot x(n - \tau) + N(n) \tag{5}$$

The waveform needs to be aligned with enough accuracy to enable symbol recovery. Common in a communication system is that a data frame is preceded by a known pilot sequence to know the exact timing of the data frame. Since we are testing system performance here it is acceptable if real data cannot be transmitted. The system design uses the transmitted waveform as a pilot to time align the received waveform. The transmitted data *x* must therefore already be known to the receiver.

To find the data frame in the received waveform, the received waveform is cross correlated with the known transmitted data. The point of maximum correlation indicates where the frame starts.

Cross correlation is defined as [14]:

$$r_{\text{yx}}(l) = \sum_{n=-\infty}^{\infty} y(n) \cdot x^*(n - l) \ . \tag{6}$$

Also, by the Cauchy-Schwarz inequality [14]:

$$\left|r_{yx}(l)\right| \leq \sqrt{E_x E_y} \tag{7}$$

where

$$E_x = \sum_{n=-\infty}^{\infty} |x(n)|^2 \tag{8}$$

is the signal energy of *x*.

Let's apply this to the problem by substituting *y* from Equation (5):

$$r_{yx}(l) = N^{'}\ (l) + \sum_{n=-\infty}^{\infty} h \cdot x(n - \tau) \cdot x^*(n - l) \tag{9}$$

where *N'* is filtered noise. It is assumed that the term N' is low compared to the sum. Comparing with (7) it is then obvious that $|r_{yx}(l)|$ reaches a maximum at $l=\tau$. Therefore, for determining the delay τ, the cross correlation is evaluated. The l giving maximum magnitude is used as an estimate of τ.

$$\hat{\tau} = \underset{l}{\operatorname{argmax}} |r_{yx}(l)| \tag{10}$$

This is easily done with MATLAB code using in-built functions as:

```
[xc,lags] = xcorr(received, transmitted);
[~, idx] = max(abs(xc));
aligned = received(lags(idx)+1:end);
```

Now the signal is time aligned and the sampling points can be determined depending on the matched filter length.

Aligning to closest sample is likely enough in a noisy system since the sample rate is 10 times the symbol rate. However, in a simulated noise-free case, time alignment to closest sample was seen to be limiting performance. So optionally, instead of the previous code, sub-sample time alignment is implemented. In that case the peak of the vector `xc` is interpolated using MATLAB's interp1(…). The maximum of the interpolated cross correlation is used to find time alignment in a similar way, but with higher time resolution than one sample. A *Thiran allpass* interpolator filter is then used to shift the signal the remaining fraction of a sample.

Symbol Sampling

When the received signal has been adjusted in time it is filtered by the same RRC pulse as used for pulse shaping, in what is called Matched Filtering. The matched filter output is downsampled to recover the transmitted symbols. The exact sampling instances are known already since the signal is time aligned with high accuracy in the previous step. It is assumed there is no remaining symbol sampling rate offsets that needs to be tracked.

The symbols are now recovered; however, the scaling of the received symbols is still incorrect. The transmitted symbols are known so the scaling of the received symbols is corrected for using a 1 tap equalizer. This is a complex number which relates the transmitted symbols to the received ones. The inverse of the equalizer is the channel coefficient providing information about attenuation and phase rotation in the channel.

Received power scales with the square of the scaling of received symbols. With this channel coefficient, h, the power of the received symbols can therefore be determined as:

$$P = 20 \cdot \log_{10}\big(\text{abs}(h)\big) + P_{\text{symbol}} \text{ [dBm]} \tag{11}$$

where P_{symbol} is a constant telling the average power received if no scaling was needed to fit the received symbols to the transmitted ones, i.e. the power received if h was 1. This was determined knowing power can be calculated from an IQ-signal given a 50Ω system as [15]

$$P_{\text{RMS}} = 10 \cdot \log_{10}\big(10 \cdot (I^2 + Q^2)\big) \text{ [dBm]}\,. \tag{12}$$

Under influence of noise and other signal degradation sources the transmitted symbols cannot be exactly recovered from the received symbols by a complex scaling factor. The offset between received and transmitted symbols can be characterized in different ways, here it will be done as Normalized Mean Square Error (NMSE). This is calculated between known transmitted symbols and received symbols after equalization as in Equation (1) of section 1.6 NMSE (Normalized Mean Square Error).

For comparison and for ensuring the signal processing is functional: during simulation of the entire signal processing chain including ΣΔ-modulation, but without any physical channel, the symbol NMSE is -60 dB.

3.2 MULTIANTENNA PROCESSING

When the single link processing was implemented the next step was to implement a multi-antenna communication system, or MIMO (Multiple Input – Multiple Output).

MIMO works by transmitting different signals from different transmit antennas. The transmit signals are carefully designed to interfere with each other in such a way that multiple data streams can be transmitted at the same time. Either each data steam is received by a dedicated antenna (MU-MIMO) or the signals from multiple receive antennas are combined in a way to enable separation of multiple streams.

The generation of these transmit signals from multiple data streams intended for different users is called precoding. There are multiple different precoding algorithms: When the transmitter knows the radio channel to all user it can use for example Zero-Forcing Precoding trying to null inter-user inference. If the channel is not known by the transmitter Blind Interference Alignment can be used to still increase rates over a SISO (Single Input Single Output) case [8]. In this project channel estimation is performed, enabling use of precoding techniques requiring channel state information (CSI).

In this system a pilot scheme was used to provide information about the radio channels for the transmitter, that is to have CSI at Transmitter (CSIT). A scope of this project was to only use a working downlink and assuming a separate perfect CSI uplink. Given these limitations it is not possible to have the mobile equipment transmit pilots and receive these at the base station. Otherwise one from these could do CSI estimation and know the downlink channel by reciprocity [2].

However using downlink pilots is not unreasonable. Simulation results in [16] showed an 18 % increase in 95 %-likely per-user throughput using downlink pilots in a low antenna density D-MIMO network.

All multi antenna processing is done under the assumption of frequency flat and non-fading channels. In such a channel each antenna path can be fully characterized just in terms of phase delay and scaling. The complex scaling from each transmit to each receiver antenna is determined and represented in the complex channel matrix *H*. Each row in *H* corresponds to a receiver antenna and each column to a transmit antenna. With this model the received signal given the transmitted signal *x* is in baseband

$$y = Hx + n \tag{13}$$

where *n* is additive noise.

The flat fading assumption sets limits on possible bandwidth. This limitation depends on conditions of the physical channel and is called coherence bandwidth. For most measurements a 2.5 Msym/s symbol rate is used in the implemented system.

3.2.1 Channel Estimation

In this system CSI estimation is done by transmitting a pilot from each antenna. It is known to the receiver what pilots were transmitted so it is possible to estimate channel effects in terms of relative phase shift and attenuation of the paths using the received waveform. Since the scheme uses only downlink pilots it is possible to have any number of receivers independently decoding the pilots and estimating CSI for that specific receiver. The goal of the channel estimation is to transmit pilots *x* and estimate the channel matrix *H* from the received waveform *y*.

There are multiple ways to design these pilots. In this implementation each pilot is generated by QAM modulating a number of magnitude 1 complex symbols, *x,* of pseudorandom phase. The symbols are spread out so that two antennas do not transmit anything at the same time, thus orthogonality is ensured. The receiver decodes the symbols and compares it with the known transmitted ones. Since there are multiple symbols per transmitter a least squares estimation of the channel matrix is performed as

$$\hat{H} = yx^H(xx^H)^{-1} \tag{14}$$

Similarly as for a single link case the average received power from each antenna during transmission is derived from each element of H as in Equation (11).

In Figure 4-2 the transmitted pilots are shown together with the received superposition of pilots. From here one can already compare the different channels in terms of received power. To see how stable this algorithm is in the intended hardware refer to section 4.1 Channel Estimation Repeatability.

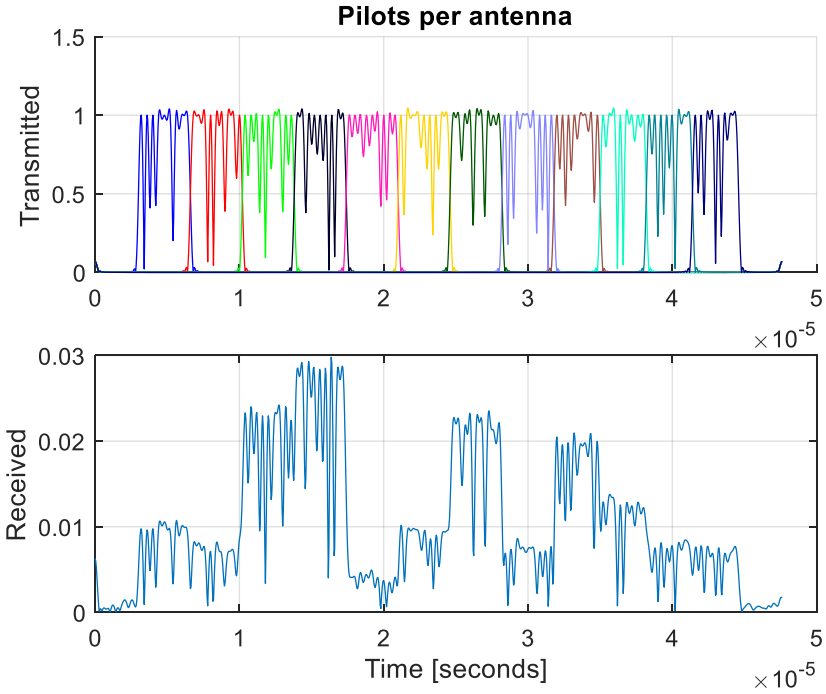

Figure 3-2: The magnitude the transmitted IQ pilots from each antenna in top figure, underneath are the received pilots in one location. Both figures are after matched filtering with the pulse shaping RRC. The y-axis scaling might not be comparable between the figures as scaling in D/A conversion etc. is not accounted for.

There is one difference between the single link transmission and the MIMO channel estimation when it comes to symbol recovery. That is in how the time alignment is done. In the single transmitter case the waveform could be time-aligned by cross correlating transmitted and received waveforms. In this case there are up to 12 transmitted pilots which must be found in the received waveform. In this case the cross correlation must be done for each pilot individually. The delay τ is assumed to be the same for all pilots, this is not necessarily true but seemed to be a reasonable approximation.

$$\hat{\tau} = \underset{l}{\operatorname{argmax}} \sum_{i=1}^{12} \left| r_{yx_i}(l) \right|. \tag{15}$$

Cross correlation is performed between the received signal and each transmitted pilot. The magnitudes of these cross correlations are summed, and the peak of this sum gives the delay. Correcting for the delay enables symbol sampling of the matched filter output.

3.2.2 Precoded Transmission

When the channel matrix is determined from the CSI estimation algorithm it can be used for precoding of data. This is implemented such as that a linear precoding matrix T is derived from the channel matrix using some algorithm. The precoding is then applied to the transmit data by multiplying the data symbols D with the precoding matrix. After that the new set of symbols are pulse shaped and upconverted just as before. This gives one signal vector per transmit antenna which are transmitted simultaneously.

On symbol level that is:

$$X = TD \tag{16}$$

Where X is a matrix of transmitted symbols as in (13). Each row of X gives symbols to transmit from one antenna. Similarly, D is a matrix with each row containing symbols for one spatial stream.

3.2.3 Beamforming

In most measurements only a single receiver was used. This case with multiple transmit antennas and only one receive antenna is called a MISO system, and precoding for such a case is called *beamforming*. In our system the power constraints are on the individual antennas and we assume full CSIT. The optimal beamforming for such a system is known and is to transmit the data from each antenna with maximum possible power but adjust the phases to add up coherently at the receiver [17]. I.e. the same symbols are transmitted from each antenna, but phase rotated to compensate for phase offsets in the channel. The precode matrix will thus be defined by

$$T_{i,j} = \frac{\overline{\widehat{H}_{j,i}}}{\left|\widehat{H}_{j,i}\right|} \tag{17}$$

where $\widehat{H}$ is the estimated channel matrix, subscripts denote matrix entry, $|\cdot|$ is absolute value and $\overline{\cdot}$ is complex conjugate. Since $\widehat{H}$ is a row vector, j=1 and T will be a column vector.

3.2.4 Zero Forcing Precoding

When multiple receive antennas are used a zero forcing (ZF) precoder is used. This is a MU-MIMO precoder, meaning that it can be used when the received waveforms are independently decoded. A ZF precoder tries to minimize inter-user interference rather than for example maximizing transmitted signal power.

The ZF precoder user in the implementation is the optimal linear ZF precoder given a sum power constraint with fair power criteria [18], i.e. the power limitation is in the total system power and we want each receiver to get the same received signal power. In our system again there is instead a per-antenna power constraint. In such a case this precoder is not anymore the optimal.

When $\widehat{H}$ is the estimated channel matrix and $\cdot^+$ is Moore-Penrose pseudoinverse, the precoder used is

$$T = \widehat{H}^+ \tag{18}$$

T is then rescaled to ensure that maximum power per antenna is not exceeded.

An issue with zero forcing precoding is that it is very sensitive to errors in the channel state information estimation. Ideally the ZF precoder nulls interference of signals destined to other users and decoding can be implemented as in the single user case.

3.3 Accuracy of CSI Estimation and Precoding

The pilot scheme combined with the channel estimation algorithm will generate a channel matrix, indicating attenuation and relative phase offset in the radio channel. This simple representation of Channel State Information (CSI) assumes a flat fading channel, where the attenuation and phase delay is constant over the signal bandwidth. Also the channel is assumed to be non-fading and not change during or between transmissions.

If the assumptions about flat fading is correct, and the CSI has been estimated correctly it would be possible to make predictions from the channel matrix. Things that could be predicted, includes Shannon limits under optimal precoding, received power using different precoders etc.

To ensure that the system functions as expected and that the channel matrix is correct some tests were performed. The received power given a specific precoder and channel conditions was analytically determined and compared to the power levels actually received during precoded transmission.

Comparing predicted and received power was done with 12 transmit antennas for a single receiver and the results are shown in Table 3. The biggest difference between predicted and actually received power is 0.7 dB.

In addition the repeatability of the channel estimation was investigated. The results of that are in the next chapter.

4 MEASUREMENTS AND RESULTS

When the hardware and software had been implemented the system could be used for channel characterization of distributed MIMO compared to co-located MIMO. Results from these measurements will be presented in this chapter. First are some tests of repeatability of the channel state information estimation.

4.1 CHANNEL ESTIMATION REPEATABILITY

To ensure system performance tests were done to verify that channel estimations were repeatable. Problems with channel estimations could possibly be seen from that multiple channel estimations in the same environment would differ. For these tests the transmitter and receiver antennas were not moved, and channel estimation was performed 600 times during a duration of 11 minutes.

The channel estimations will only give relative phase offsets between the different channels. Therefore, each of the 600 received channel vectors were rotated to match each other in a LSE sense. The channel estimations are visualized in Figure 4-1 in terms of received power and relative phase offset.

In the figure a high consistency between channel estimates is seen since the 600 points of a measured path are close. The standard deviation of the phase estimation was below 2.7 degrees for each channel and 0.03 dBm in the power estimation (variance calculated from values in dBm).

It is unknown if the channel estimation differences are due to non-idealities in the channel estimation algorithm, effects from white- or phase noise or represents actual changes in the channel due to other unknown effects between measurements. To quantify how the difference influences beamforming performance it is assumed that the first channel estimate is used for beamforming during all the later experienced channels. The received power in these cases is determined analytically and presented as a histogram in Figure 4-2. The differences in experienced channels gives only a small difference in received power supporting that the channel estimate differences can be considered small.

During these measurements the CFO was measured as determined according to method in section CFO Compensation.

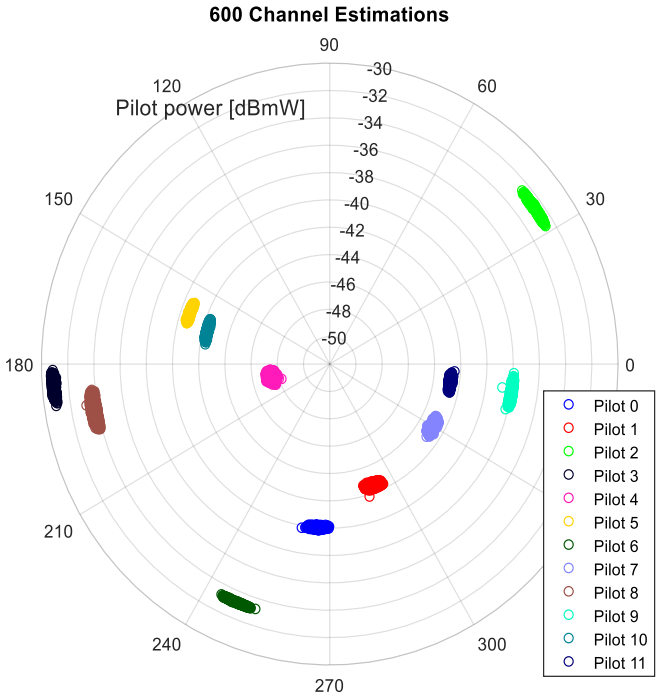

Figure 4-1: Results of N=600 channel estimations within 11 minutes. The channels are represented by relative phase and received power from each received pilot. 12 transmit antennas were used.

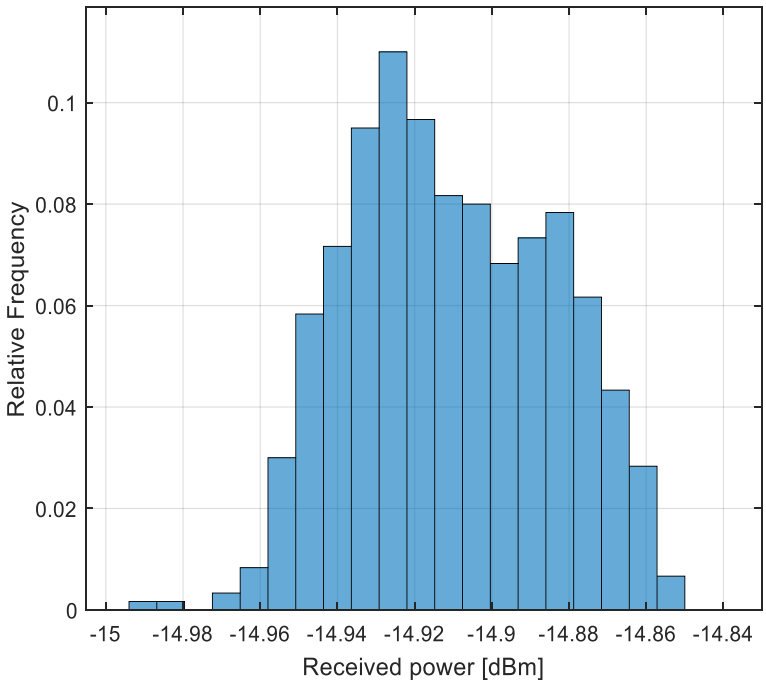

Figure 4-2: Histogram of: N=600 estimates of received power given a constant precoder in a supposedly unchanging channel. Standard deviation (not in dB) is 0.2 μW and average received power is 32.3 μW.

4.2 MISO MEASUREMENTS

The assumed differences between distributed MIMO and co-located MIMO were in terms of coverage as well as lower correlation between channels in a multiuser case. In this section a single user has been used and coverage investigated.

There were measurements of the channel matrices as well received power during beamforming at multiple locations in a lab environment. The receiver is in this case was a sampling oscilloscope moveable on wheels. The receiver used an omnidirectional antenna which is positioned about 115 cm above the floor.

The antennas were placed either taped to the walls, ceiling or placed on top of cabinets. The antenna vertical location therefore differed with an average of 220 cm above the floor. Figure 4-3 shows one of the RRHs position.

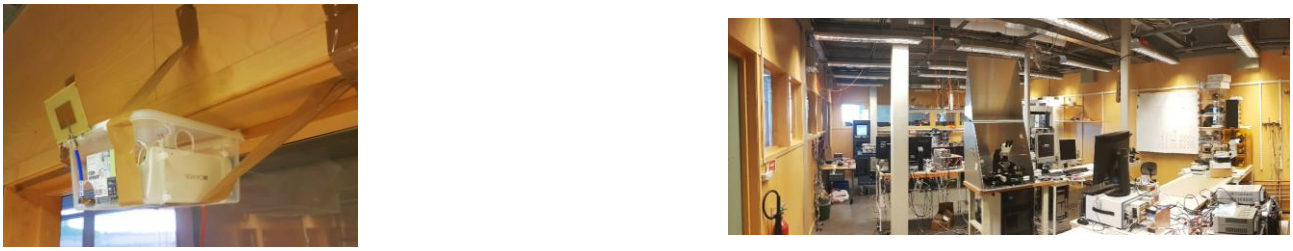

Figure 4-3: The placement of one of the wall mounted RRHs (left image). The measurement room (right).

4.2.1 12 Antennas Distributed

All the 12 antennas were placed along the walls in a lab room, i.e. a scatter rich environment. In this environment the receiver was moved around. Channel estimation was done at 24 locations in the room followed by beamforming to that location. Figure 4-4 shows received power at different parts of the room.

For comparison, the power that would have been received without beamforming is presented. This is received power if only one transmit antenna had been used but with 12 times the transmit power. To calculate this the received power from the strongest antenna times 12 is shown. In all test locations it is more beneficial to use beamforming than to use a single transmit antenna at equivalent transmit power.

This shows the advantage of using beamforming, with the same total transmit power the received power is higher at the receiver using it. Beamforming achieves a similar effect as having a directed antenna. Another way of seeing this is that signals are added in voltage instead as in power, and having 12 times the voltage corresponds to having 144 times the power.

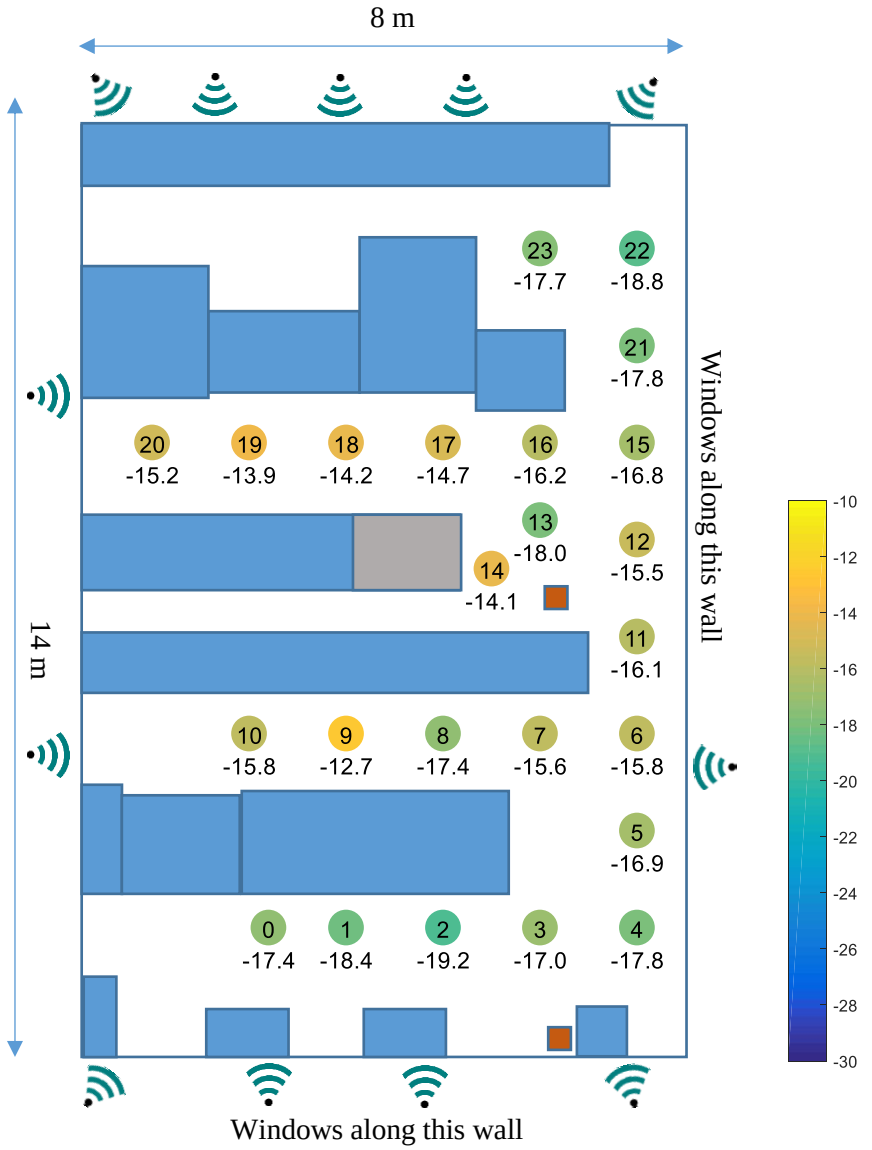

Figure 4-4: Antenna locations and received power under beamforming in different locations of a room, each measurement location has a number for referencing Table 3. Received power values are written on the measurement points and given in dBm. Measurement point color also indicates received power given the color map to the right. The squares represents objects in the room – blue are tables, gray is metal object and brown are pillars.

Some analysis was done to ensure system functioning and that the CSI was correctly determined. Since the channel matrix is now determined it is possible to analytically calculate the power that will be received after beamforming. This was calculated for comparison with the actually measured power, where any differences would indicate that the CSI was incorrect.

This is presented in Table 3 for the distributed case.

Table 3: Power analysis of data from 12 transmitters. The actual received power after beamforming, the power expected to be received after beamforming, the power that would be received if only the best antenna were to transmit but with 12 times the power. All powers in dBm. There is also the NMSE (dB) of the received constellation during actual beamformed transmission. The measurement locations can be seen in Figure 4-4.

	Measured during beamforming		Derived from H-matrix	
Location nr.	Received Power Beamforming	NMSE Received (dB)	Expected Power Beamforming	Best Channel Comparable Power
0	-17.4	-27.0	-17.3	-23.2
1	-18.4	-26.7	-18.3	-22.3
2	-19.2	-26.0	-18.5	-20.9
3	-17.0	-28.3	-17.4	-21.6
4	-17.8	-26.8	-17.7	-20.7
5	-16.9	-26.5	-16.8	-20.5
6	-15.8	-25.6	-16.2	-22.0
7	-15.6	-27.3	-15.3	-21.0
8	-17.4	-27.2	-17.1	-22.6
9	-12.7	-27.0	-12.4	-14.7
10	-15.8	-27.1	-16.0	-18.7
11	-16.1	-26.9	-15.9	-19.7
12	-15.5	-26.7	-15.3	-21.0
13	-18.0	-25.3	-17.6	-18.6
14	-14.2	-27.2	-14.3	-17.3
15	-16.8	-27.2	-16.9	-17.5
16	-16.2	-26.9	-16.3	-19.7
17	-14.7	-27.0	-14.8	-19.3
18	-14.2	-26.7	-14.4	-16.2
19	-13.9	-26.1	-13.9	-15.6
20	-15.2	-26.2	-15.4	-18.5
21	-17.8	-26.0	-17.7	-20.5
22	-18.8	-27.1	-19.1	-23.6
23	-17.7	-26.5	-17.6	-21.3
Median:	-16.5	-26.85	-16.55	-20.5
Mean:	-16.3	-26.7	-16.3	-19.9

4.2.2 12 Antennas Co-Located

A similar measurement sequence was done when the antennas instead were placed closely as to simulate a co-located system. Results and antenna positions shown in Figure 4-5. The received power can be compared to the received power in the distributed set-up by the histograms in Figure 4-6, the histograms contain the data as the map figures.

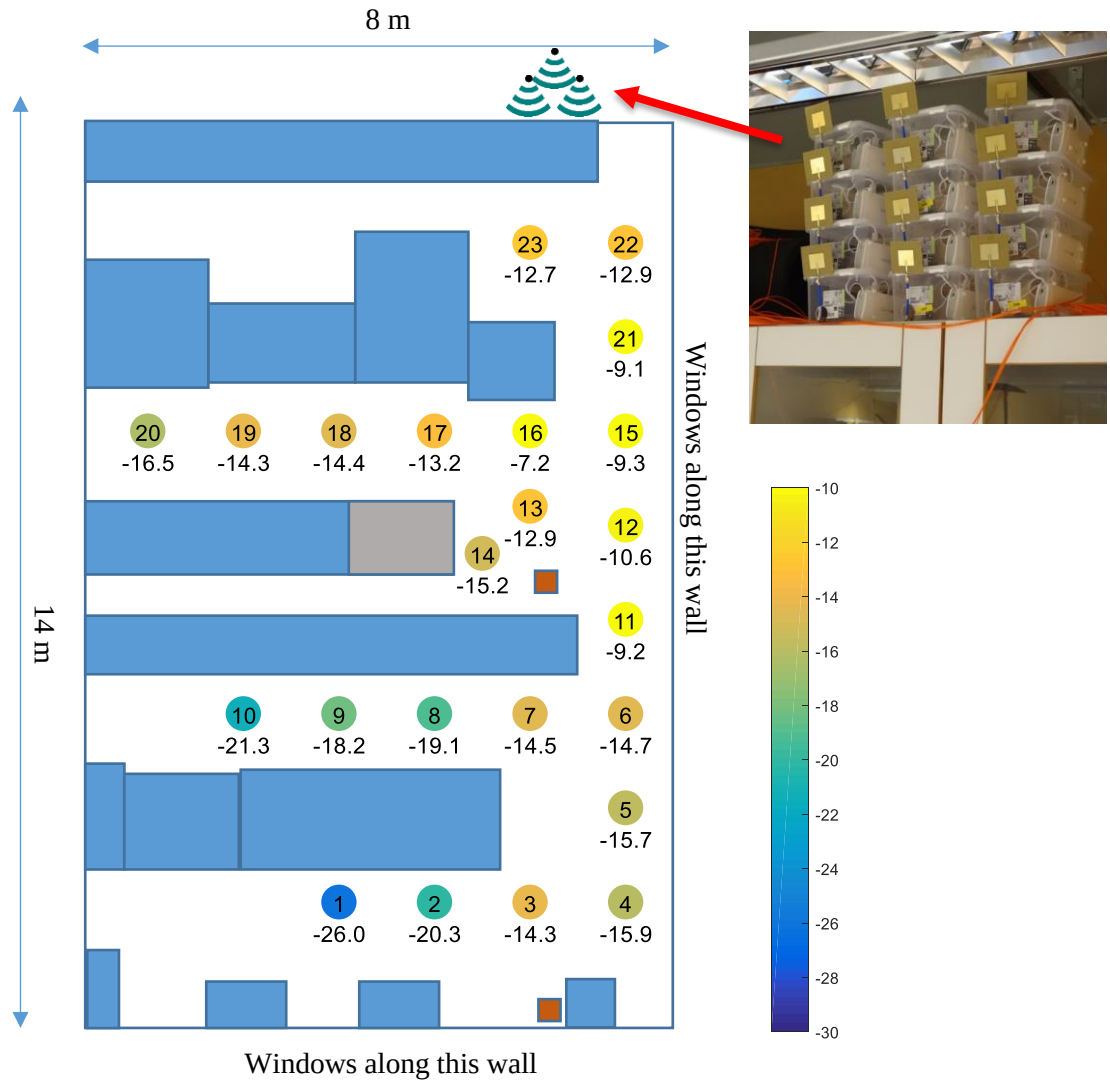

Figure 4-5. Received power under beamforming in different locations of a room. Received power values are written on the measurement points and given in dBm. Measurement point color indicates received power given the color map to the right. The antenna placement is shown in top-right.

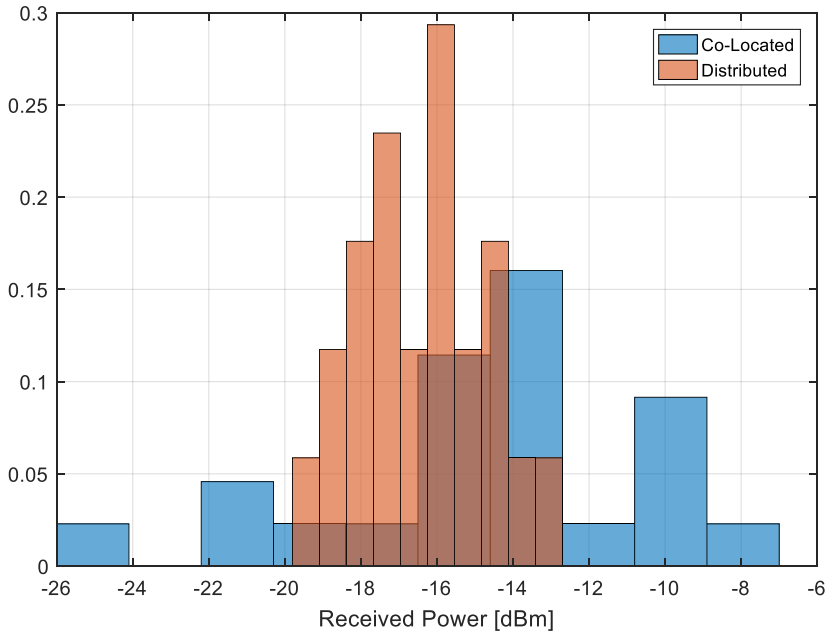

Figure 4-6: 10 bin histograms over received power for both co-located and distributed antenna set up.

4.3 MIMO MEASUREMENTS

Tests were performed ensuring that the test bed works for MIMO transmission. These tests were performed with Zero Forcing precoding as explained in Section 3.2.4. Four receiver locations were used for both a distributed and co-located antenna set-up as in the previous chapter.

Apart from testing precoding to all four receivers, tests were performed with three as well as two receivers. Using these four locations there were thus 11 possible antenna selections which were all tested.

A limitation was that only one receiver (the spectrum analyzer in IQ-mode) was available and MIMO by definition uses multiple receivers. To overcome this issue a multi-receiver system was simulated using the single receiver as follows.

1. 4 receive antennas are placed in a room.
2. The receiver hardware is moved between the different antennas and channel conditions are estimated in each location creating a channel matrix.
3. This channel matrix is used to design zero-forced precoded data transmission.
4. The receiver hardware is moved between the receive antennas and the incoming waveforms are sampled in each location.
5. Signal properties are determined in terms of NMSE.

If the channel conditions did not change between measurements in step 2 and step 4 the received waveforms should be the same as if multiple receivers had been used simultaneously.

This test was seen to be harder to accomplish than expected. The received antennas were taped in place, but the experienced channel kept changing between channel estimation and precoded transmission. To mitigate the issues the antennas were placed close to each other so the active receive antenna could be changed by only moving the cable from the antenna to the receiver. In the final tests the antennas were placed just a few decimeters apart as seen in Figure 4-7.

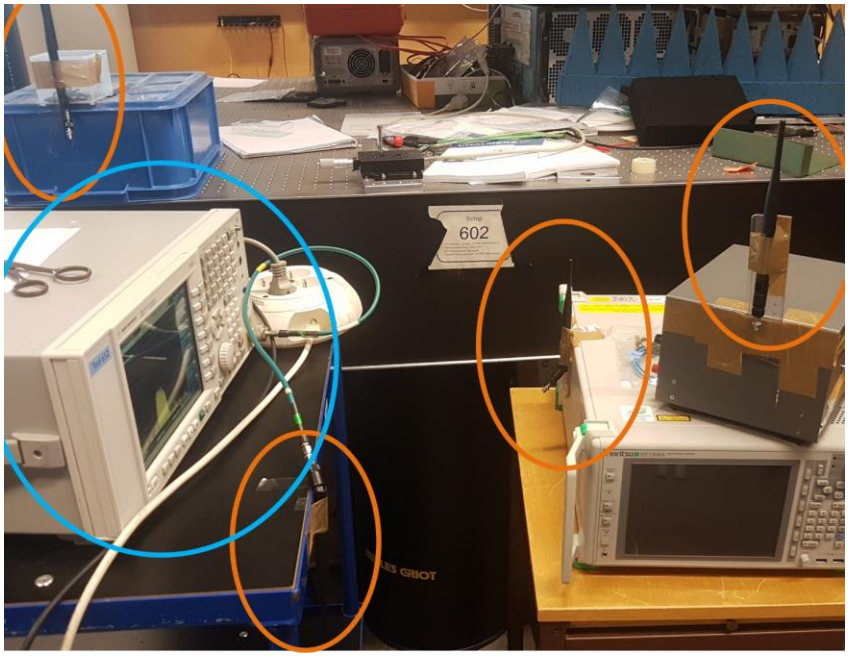

Figure 4-7: The four receiver antennas during MIMO tests are circled in orange. Only one antenna is connected at the time to the receiver circled in blue.

The results of the tests are shown in Figure 4-8 – 4.9. In these figures the received power as well as the NMSE of the received waveform is plotted. There are 11 transmissions for each transmit antenna set-up. One where all four receivers are used for precoding and one for each combination of two or three receive antennas. In the figures all results have been plotted with a single line for each measurement – note again that not all measurements involve all receivers.

For example, for three active receivers there are four different measurements. One where each of the possible four receivers are turned off and not used for precoding. That is the reason for the four lines in the 3 receivers plot. The green line in the 3 receivers-plot show NMSE and received power when using ZF precoding to receiver 1, 3 and 4.

The reason for the high NMSE in some locations are not fully understood. It is likely due to interference, possibly due to bad channel state information. This would likely be a combination of problems keeping the receivers stable between channel estimation as well as that the CSI estimation is imperfect.

Also a zero-forcing precoder is used. There are other precoders and scheduling algorithms that could potentially give better performance. Due to the few data samples gathered together with the other issues no conclusions about performance of a distributed versus co-located antenna set up can be drawn.

The highest NMSE measured was -13 dB for four receivers and the co-located antenna set-up which is already useful for communication. These tests show that the testbed is useful for achieving spatial multiplexing and is therefore a demonstration of distributed MIMO using SDoF.

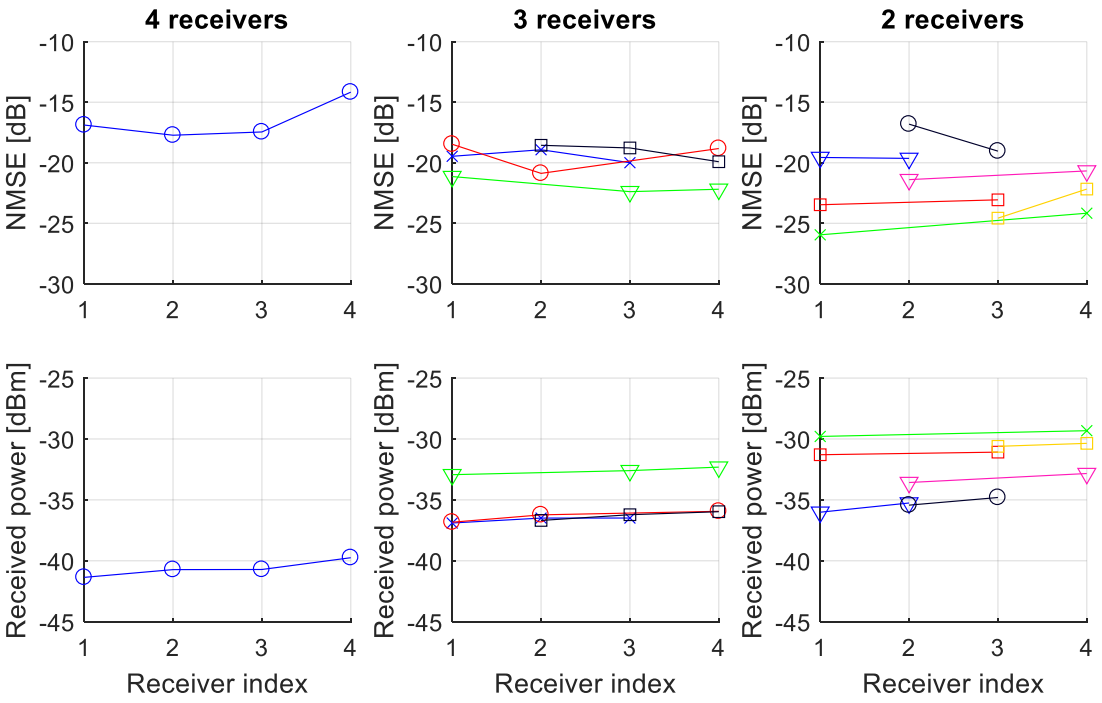

Figure 4-8: Results of received power and NMSE during zero-forcing precoding and a distributed transmit antenna set-up. During the 11 tests two to four of the receivers were activated and used for precoding at a time. A marker placement in the graphs indicates that the corresponding receiver was active during measurement.

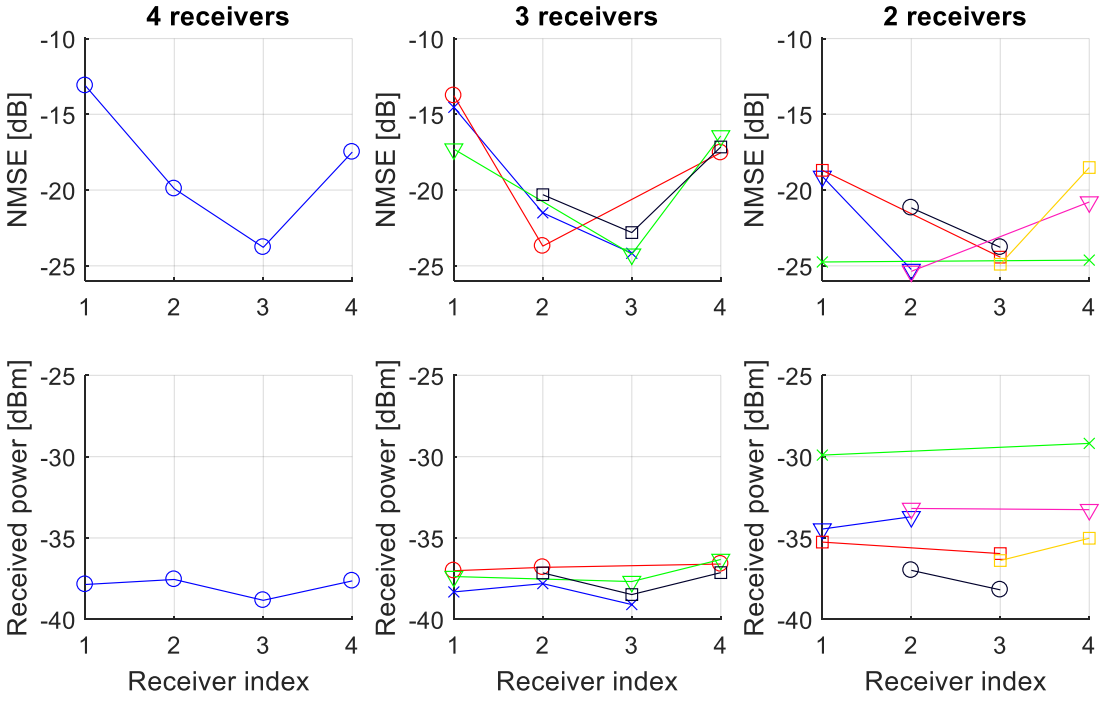

Figure 4-9: Results of received power and NMSE during zero-forcing precoding and a co-located transmit antenna set-up. During the 11 tests two to four of the receivers were activated and used for precoding at a time. A marker placements in the graphs indicates that the corresponding receiver was active during measurement.

In future test of similar nature an RF switch could be used to lower the time to switch between different receivers and for avoiding the movements of connecting and disconnecting coaxial cables. Another way would be to have more physical receivers and do MIMO tests with simultaneous receiving.

5 CONCLUSION

In this thesis a testbed was developed which enabled phase coherent transmission from distributed transmit antennas. It was seen that the testbed gave consistent CSI estimates of a distributed downlink antenna setup and that these estimates could be used to precode transmissions.

The development of this testbed included communication system software development in MATLAB and hardware design of antennas and PCBs.

Tests were performed using a single receiver with 12 transmitters beamforming a signal, i.e. transmitting phase rotated versions of the signals so that these add coherently at the receiver. Received signal in tests had a normalized mean square error (NMSE) below -26 dB. These tests where done with a 2.5 MSym/s 16-QAM transmission at 2.365 GHz carrier frequency. They were performed in a scatter-rich lab environment with both a distributed and co-located antenna set up.

Some indications for better performance with a distributed antenna set-up were seen in terms of coverage. There is not enough measurement data gathered to draw any final conclusions of the gains of D-MIMO.

In addition to the single receiver (MISO) measurements there were measurements performed with multiple receivers (MIMO). These measurements were performed using zero-forcing precoding and only a single physical receiver moved between measurement points. For a distributed antenna set-up for four receiver locations the NMSE was measured to be below -14 dB.

The MIMO measurements method had some drawbacks and likely the signal quality could be further increased with more complex precoders as well as by further ensuring a non-changing channel between measurements.

The developed testbed could be used for more research. Within the time frame of this thesis most effort was spent in software and hardware design as well as hardware assembly. With more time more measurement data could be gathered. This would be needed to draw conclusions of if distributed MIMO has any advantages over co-located MIMO. Also since most signal processing is done in digital domain tests at other signal parameters could be performed, for example with higher bandwidths using OFDM.

6 REFERENCES

[1] H. Zhang and H. Dai, "On the Capacity of Distributed MIMO Systems," in *Proc. Conf. Inform. Sciences and Systems (CISS)*, Princeton University, 2004.

[2] A. Ashikhmin, H. Yang, E. G. Larsson and T. L. Marzetta, "Cell-Free Massive MIMO Versus Small Cells," *IEEE Transactions on Wireless Communications,* vol. 16, no. 3, pp. 1834 - 1850, 19 January 2017.

[3] K. Zhu, M. J. Crisp, S. He, R. V. Penty and I. H. White, "MIMO system capacity improvements using radio-over-fibre distributed antenna system technology," in *2011 Optical Fiber Communication Conference and Exposition and the National Fiber Optic Engineers Conference*, 2011.

[4] Q. Cui, H. Wang, P. Hu, X. Tao, P. Zhang, J. Hamalainen and L. Xia, "Evolution of Limited-Feedback CoMP Systems from 4G to 5G: CoMP Features and Limited-Feedback Approaches," *IEEE Vehicular Technology Magazine,* vol. 9, no. 3, pp. 94-1033, 2014.

[5] L. M. Pessoa, J. S. Tavares, D. Coelho and H. M. Salgado, "Experimental evaluation of a digitized fiber-wireless system employing sigma delta modulation," *Opt. Express,* vol. 22, no. 14, pp. 17508-17523, July 2014.

[6] Artemis Networks LLC, "An Introduction to pCell, White Paper," 2015.

[7] Ericsson, "5G live test demo: Multipoint Connectivity with Distributed MIMO," [Online]. Available: https://www.youtube.com/watch?v=jCO68dPoNwA.

[8] H. Vlad Balan, R. Rogalin, M. Antonios, P. Konstantinos and C. Giuseppe, "Achieving high data rates in a distributed MIMO system," in *Proceedings of the 18th annual international conference on Mobile computing and networking*, 2012.

[9] E. Hamed, H. Rahul, M. A. Abdelghany and D. Katabi, "Real-time distributed MIMO systems," in *Proceedings of the 2016 ACM SIGCOMM Conference*, Florianopolis, Brazil, 2016.

[10] S. Pavan, R. Schreier and G. C. Temes, Understanding Delta-Sigma Data Converters, John Wiley & Sons, 2017.

[11] A. Goldsmith, Wireless Communications, Cambridge University Press, 2005.

[12] M. Natsir, "Cst training core module - antenna - (2)," [Online]. Available: https://www.slideshare.net/bundahamka/cst-training-core-module-antenna-2?next_slideshow=1. [Accessed 31 05 2018].

[13] P. J. Bevelacqua, "Antenna-Theory: Rectangular Microstrip Antenna," [Online]. Available: http://www.antenna-theory.com/antennas/patches/antenna.php. [Accessed 31 05 2018].

[14] J. Fessler, "Discrete-time signals and systems," in *Lecture notes*, 2004.

[15] Tektronix, "Calculating RF Power from IQ Samples," [Online]. Available: https://www.tek.com/blog/calculating-rf-power-iq-samples. [Accessed 27 May 2018].

[16] G. Interdonato, H. Q. Ngo, E. G. Larsson and P. Frenger, "How much do downlink pilots improve cell-free massive MIMO?," in *Global Communications Conference (GLOBECOM), 2016*, 2016.

[17] M. Vu, "MISO Capacity with Per-Antenna Power Constraint," *IEEE Transactions on Communications,* vol. 59, no. 5, pp. 1268-1274, 2011.

[18] A. Wiesel, Y. C. Eldar and S. Shamai, "Zero-Forcing Precoding and Generalized Inverses," *IEEE Transactions on Signal Processing,* vol. 56, no. 9, pp. 4409-4418, 2008.

[19] "Receiver Sensitivity and Equivalent Noise Bandwidth," [Online]. Available: https://www.highfrequencyelectronics.com/index.php?option=com_content&view=article&id=553:receiver-sensitivity-and-equivalent-noise-bandwidth&catid=94:2014-06-june-articles&Itemid=189.

APPENDIX: LINK BUDGET FORMULAS

A link budget connects transmitted power and received power between two antennas taking losses and antenna directivity into account. The simplest model is the free space path loss model, assuming two antennas communicating in free space. [11]

$$\frac{P_r}{P_t} = \left[\frac{\sqrt{G_t G_r}\lambda}{4\pi d}\right]^2 \tag{19}$$

where P_r and P_t are received respectively transmitted signal power. G_t and G_r are antenna gains of transmit and receive antennas. d is distance between the antennas and λ is carrier frequency. Note that this equation is in linear scale and not in logarithmic.

The receiver sensitivity is the minimum input power that is needed to demodulate a signal [19]

$$P_{r,\text{min}} = 10 \cdot \log_{10}(kTb) + NF + \text{C/N [dBW]} \tag{20}$$

$P_{r,\text{min}}$ is receiver sensitivity, k is the Boltzmann constant (k=1.38e-29 J/K), T is the operating temperature in Kelvin, b is the signal bandwidth, NF is Noise Figure, which represents degradation in SNR compared to an ideal receiver and C/N is the wanted carrier-to-noise ratio or SNR.

With these two equations the minimum transmit power to reach a certain signal-noise-ratio is found. To that some margin should be added to account for e.g. deviations from the free space model in other environments.